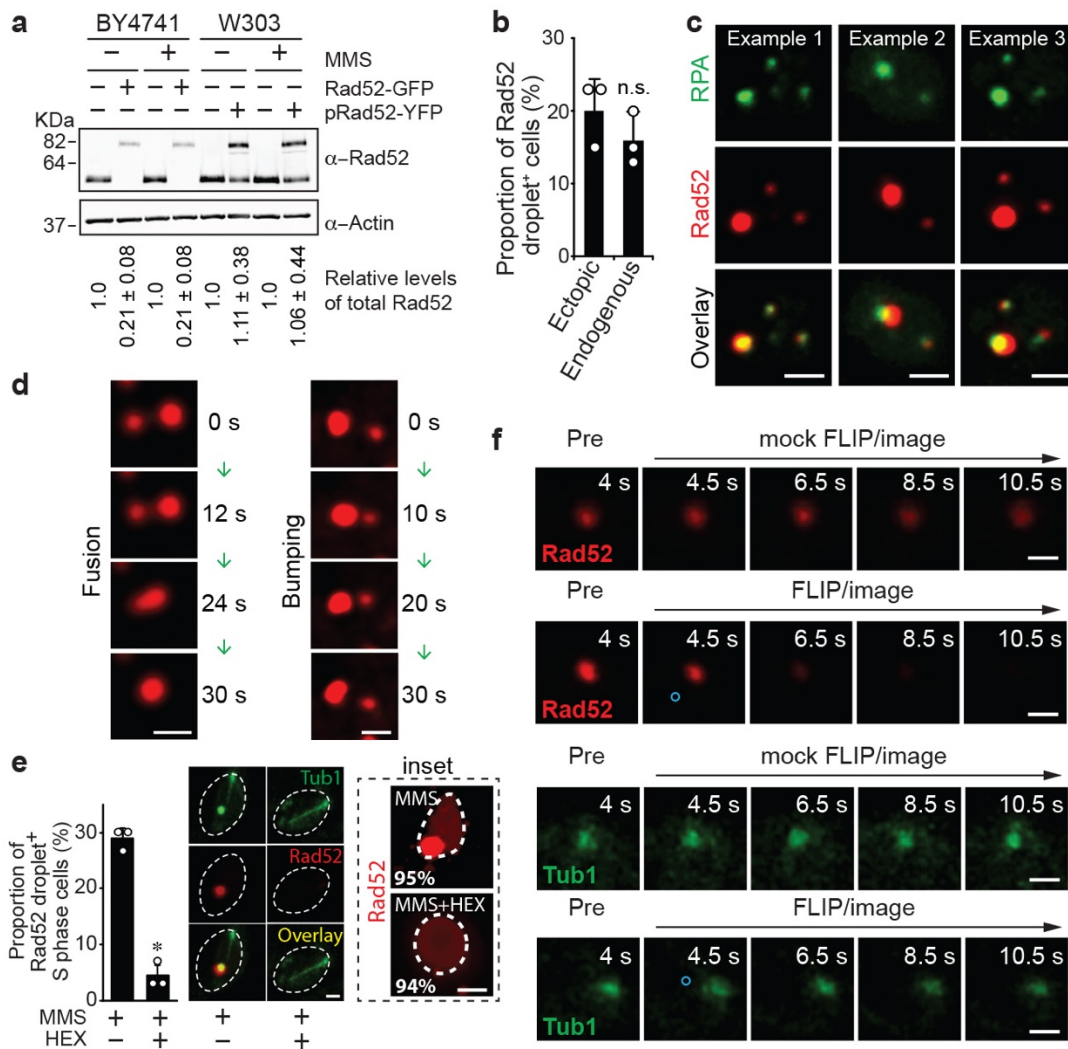
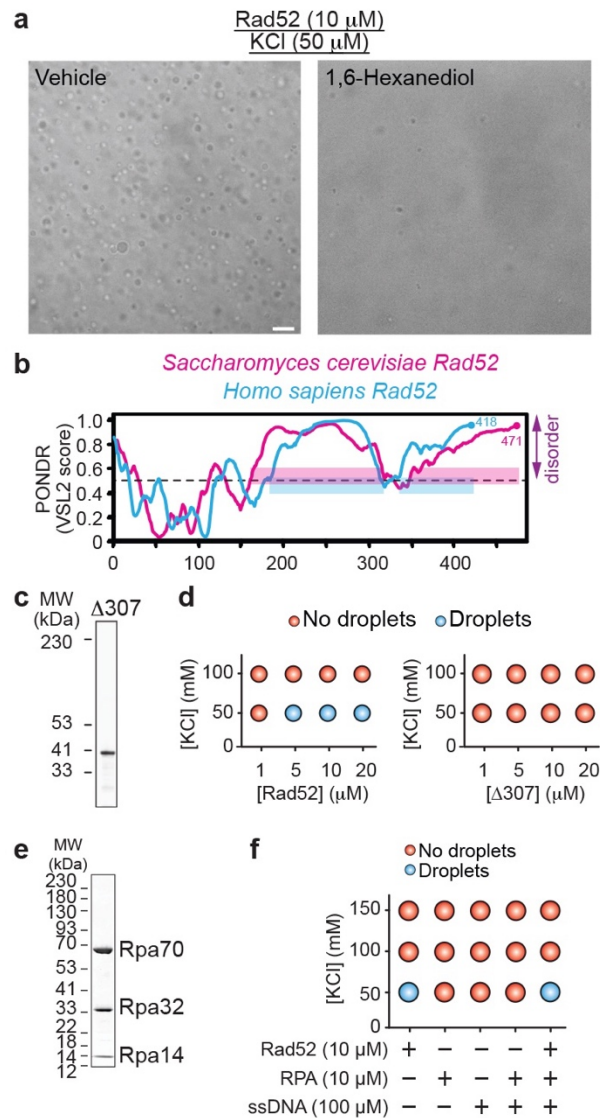


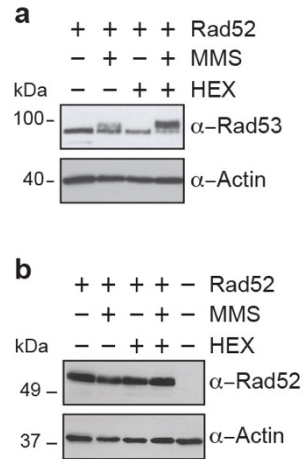
Supplementary Information



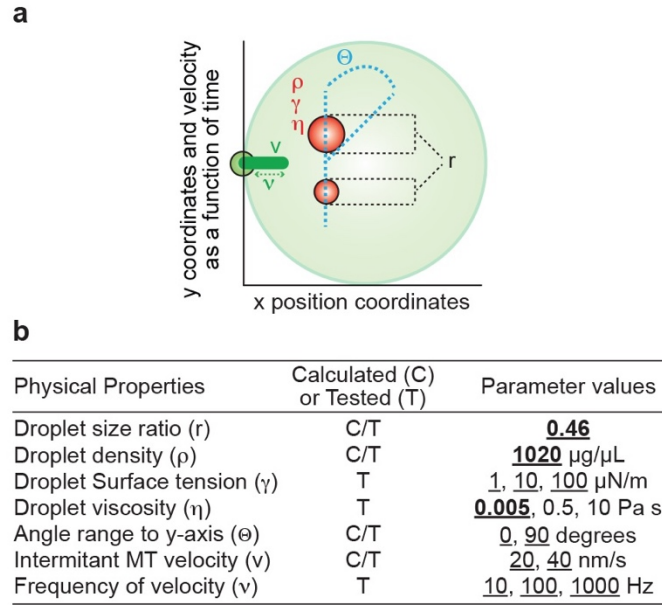
Supplementary Figure 1 | DSB-inducing Rad52 foci behave like liquid droplets *in vivo*. **a-b**, Plasmid-borne expression of fluorescently labelled Rad52, but not endogenously tagged Rad52, preserves total Rad52 protein levels (**a**) and MMS-induced Rad52 focus formation is similar when Rad52 is endogenously or exogenously tagged (**b**). Quantifications and standard deviations of total Rad52 protein levels in each lane normalized to its respective untagged control from three independent experiments are presented below the blots. **c**, Live cell microscopy shows that all Rad52 foci observed associate with an RPA focus ($n=3$, 251 foci). **d**, Zeocin-induced Rad52 droplets exhibit liquid droplet behaviours (scale bar, 0.5 μM). **e**, 1,6-Hexanediol disrupts Rad52 liquid droplets ($n=3$, 120 cells). Inset: 1,6-hexanediol disrupts MMS-induced Rad52 foci without altering the percentage of Rad52 fluorescence that is associated with the nucleus (dashed outline). (scale bar, 0.5 μM). **f**, Representative images of Rad52-YFP and GFP-Tub1 signal loss during FLIP experiments. Scale bars, 1 μM . Quantifications represent the mean \pm s.d.; * $P < 0.0001$ in χ^2 test.



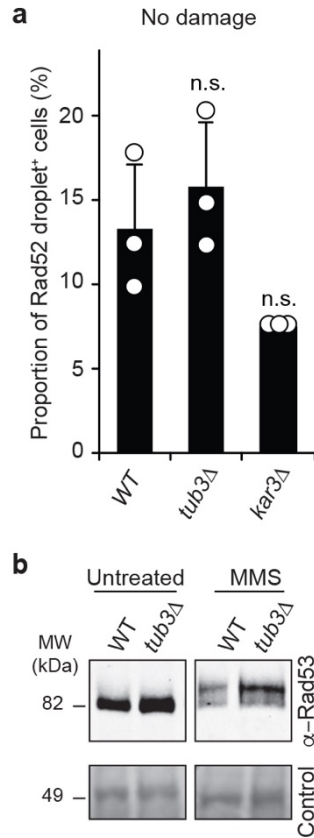
Supplementary Figure 2 | Factors that influence Rad52 phase-separation *in vitro*. **a**, Addition of 1,6-Hexanediol disrupts pre-formed Rad52 liquid droplets *in vitro*. Scale bar, 10 μ m. **b**, Predictor of Natural Disordered Regions (PONDR) reveals that yeast and human Rad52 display similar disorder profiles across their amino acid sequences. **c-d**, Purified Rad52 C-terminal truncation Δ 307 fails to form droplets *in vitro*. **e-f**, Addition of RPA in complex with ssDNA does not influence Rad52 phase separation at varying salt concentrations.



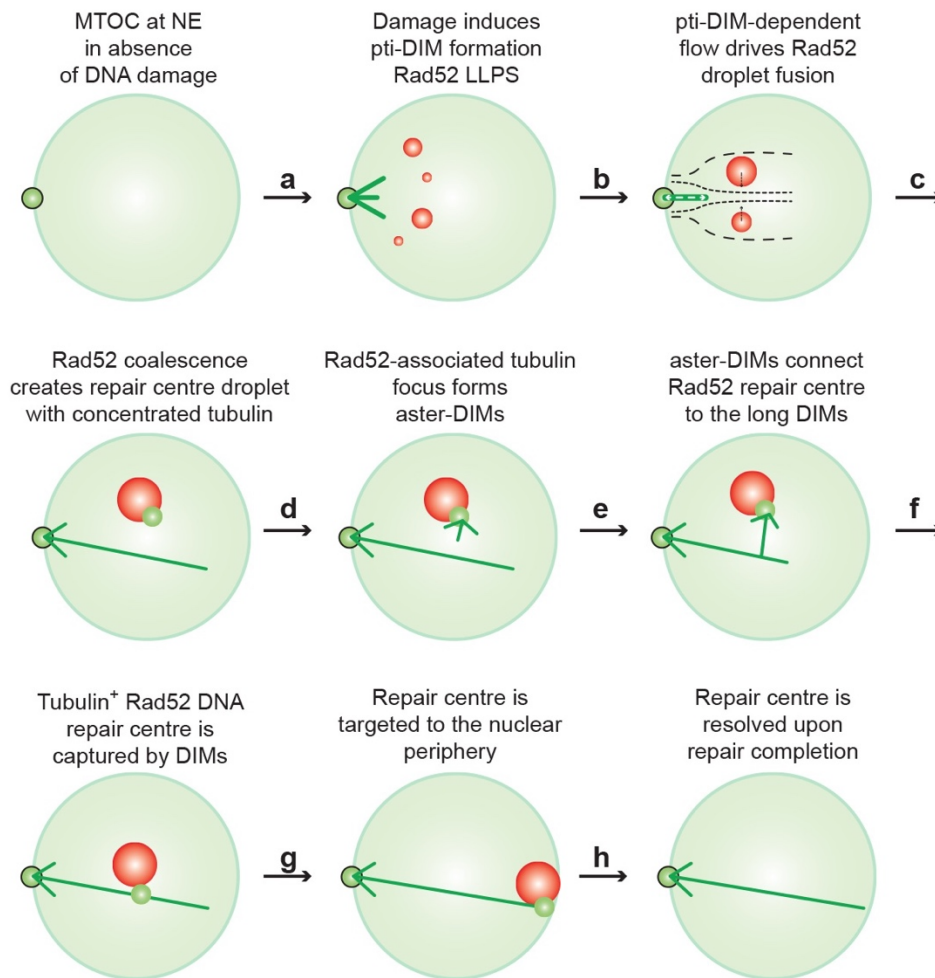
Supplementary Figure 3 | Phase-separation disruptor 1,6-Hexanediol hyper-activates the DNA damage checkpoint only in the presence of DNA damage induction. a-b, Treatment with 1,6-Hexanediol (HEX) leads to hyperactivation of the Rad53 DNA damage checkpoint protein only in the presence of MMS (**a**) without altering cellular Rad52 protein levels (**b**).



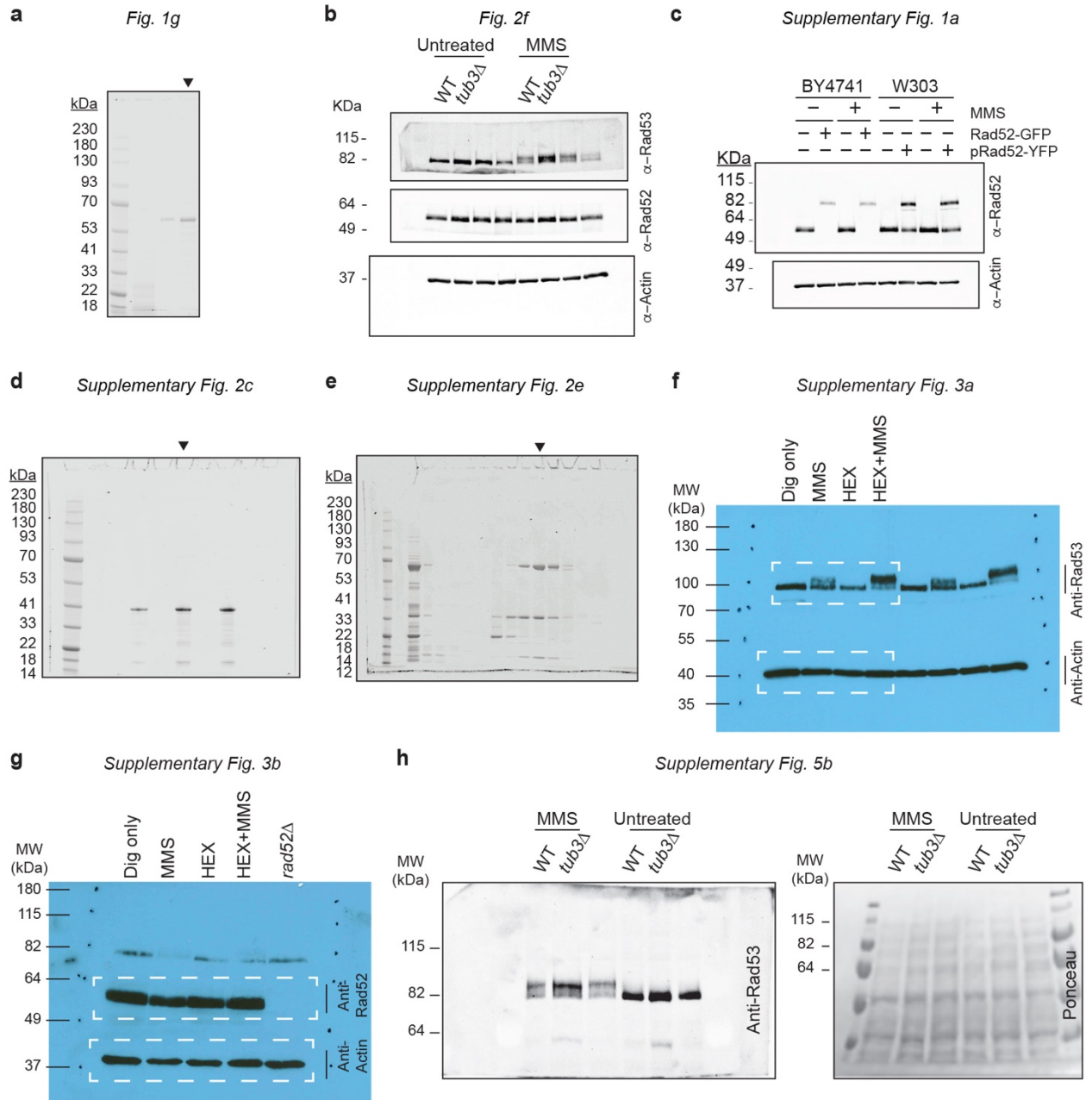
Supplementary Figure 4 | Parameters of CFD simulations of Rad52 liquid droplet fusions. **a-b**, Schematic (**a**) and list (**b**) illustrating key parameters incorporated in the CFD simulations. Parameter values underlined are compatible with fusion while those bolded result in the most efficient fusion kinetics.



Supplementary Figure 5 | Endogenous levels of Rad52 droplets. **a**, Quantification of Rad52-YFP droplets via live-cell microscopy. Quantifications represent the mean \pm s.d.; χ^2 test was used. **b**, Longer running gel electrophoresis followed by western blotting shows that Tub3 deletion induces a higher migrating band indicating Rad53 hyper-phosphorylation. Ponceau serves as loading control.



Supplementary Figure 6 | Model. Upon the induction of multiple DNA breaks, the evolutionarily conserved Rad52 protein assembles liquid droplets (red spheres) at the sites of DNA damage across the nucleus (large faint green sphere) (a). Novel intranuclear filaments termed pti-DIMs (short green sticks) also emerge from the nuclear envelope-embedded MTOC (a). Extension-shortening motions of pti-DIMs can then create a nucleoplasmic flow driving the fusion of the separate Rad52 droplets into a DNA repair centre droplet (b, c). The repair centre droplet internally concentrates tubulin and projects novel aster-like nuclear filaments termed aster-DIMs (c, d). One of the latter filaments matures and allows the Rad52 repair centre droplet to be captured by a long DIM (e, f) for mobilization to the nuclear periphery for repair (g, h). MTOC, microtubule organizing centre; NE, nuclear envelope; pti-DIMs, petite DNA damage-inducible intranuclear microtubule filaments; LLPS, liquid-liquid phase separation; aster-DIMs, aster-like DNA damage-inducible intranuclear microtubule filaments.



Supplementary Figure 7 | Uncropped SDS-PAGE gels and immunoblots. Uncropped gels and immunoblots related to indicated main and supplementary figure panels.

Supplementary Table 1 | List of *S. cerevisiae* strains and plasmids used in this study.

| Reagent | Genotype | Source |
|-----------------|--|-----------------------------|
| KMY 2559 | W303 MATa ade2-1 trp1-1 can1-100 leu2-3,112 his3-11,15 ura3-1 GAL+ psi+ ssd1-d2 RAD5+ | This study |
| KMY 372 | BY4741 MATa his3Δ1 leu2Δ0 met15Δ0 ura3Δ0 | This study |
| KMY 3426 | W303 MATa ade2-1 trp1-1 can1-100 leu2-3 URA3 GFP-Tub1-HIS3 nup49-GFP-KanMX pKM199-(Rad52-YFP-TRP1) | This study |
| KMY 3557 | BY4741 Rfa1-GFP-HIS3+ pKM201 (Rad52-YFP-LEU2) | This study |
| KMY 3542 | BY4741 Rad52-GFP-HIS3 | Kind gift from Brown lab |
| KMY 3581 | KMY 3426 tub3Δ::HphR | This study |
| KMY 3459 | KMY 3426 kar3Δ::HphR | This study |
| KMY 3587 | KMY 3426 htz1Δ::HphR | This study |
| pKM199 | Rad52-YFP-TRP1 | Kind gift from Durocher lab |
| pKM 201 | Rad52-YFP-LEU2 | This study |
| pKM397 | (His)6-RAD52(N+M)::pET11d | Kind gift from Krejci lab |
| pKM 412 | (His)6-RAD52Δ307 (N+M)::pET11d | This study |
| pKM 403 | p11d-sctRPA | Addgene |